Optics Letters

Continuous cubic phase microplates for generating high-quality Airy beams with strong deflection

Ze Cai,[1] Ya Liu,[2] Chenchu Zhang,[1] Jiangchuan Xu,[3] Shengyun Ji,[1] Jincheng Ni,[1] Jiawen Li,[1] Yanlei Hu,[1,4] Dong Wu,[1,5] and Jiaru Chu[1]

[1]CAS Key Laboratory of Mechanical Behavior and Design of Materials, Department of Precision Machinery and Precision Instrumentation, University of Science and Technology of China, Hefei, Anhui 230027, China
[2]Department of Precision Machinery and Precision Instrumentation, University of Science and Technology of China, Hefei, Anhui 230027, China
[3]Laboratory of Supervisory Control and Data Acquisition, Department of Precision Machinery and Precision Instrumentation, University of Science and Technology of China, Hefei, Anhui 230027, China
[4]e-mail: huyl@ustc.edu.cn
[5]e-mail: dongwu@ustc.edu.cn

Received 7 April 2017; revised 24 May 2017; accepted 28 May 2017; posted 30 May 2017 (Doc. ID 292185); published 21 June 2017

Owing to the distinguishing properties of nondiffraction, self-healing, and transverse acceleration, Airy beams have attracted much attention in the past decade. To date, a simple approach for exquisitely fabricating cubic phase plates with both continuous variation of phase and micro size still remains challenging, which limits the generation of high-quality Airy beams for integrated micro-optics. Here, we report the elaborate design and fabrication of a continuous cubic phase microplate (CCPP) for generating high-quality Airy beams in micrometer scale. A CCPP with a precise size (60 μm × 60 μm × 1.1 μm) is fabricated by femtosecond laser direct writing, exhibiting a high optical efficiency (∼79%). The high-quality Airy beam generated via the CCPP demonstrates an unprecedentedly strong deflection (∼4.2 μm within a 90 μm propagation distance) as well as being diffraction-free. Our research on the design and fabrication of miniature Airy phase plates paves the way toward high-performance integrated optics, optical micromanipulation, and optical imaging.

OCIS codes: (140.3390) Laser materials processing; (220.4000) Microstructure fabrication; (100.5090) Phase-only filters; (130.3990) Micro-optical devices; (350.5500) Propagation.

https://doi.org/10.1364/OL.42.002483

Since Airy beams were experimentally demonstrated by Siviloglou and coworkers in 2007 [1,2], a variety of theoretical and practical research has emerged. Thanks to the distinguishing properties of nondiffraction, self-healing, and transverse acceleration, Airy beams have exhibited various applications such as optical micromanipulation of particles [3,4], spatiotemporal Airy light bullets [5], generation of curved plasma channels in air [6], surface plasmons control [7,8], laser micromachining of curved structures [9], generation of electron Airy beams [10], and microscopy [11,12].

Up to now, the most common method to generate Airy beams has been based on Fourier-transform-type modulation realized by spatial light modulators (SLMs) [1]. Unfortunately, the optical efficiency of SLMs is relatively low (∼40%), because typical SLMs consist of numerous discrete micro-size pixels driven by a complex electrode matrix [13]. Binary cubic phase patterns executed by liquid crystals (LCs) like polymer-dispersed LCs [14] and polymer-stabilized LCs [15] have been utilized to generate Airy beams as well. However, it is disappointing that two Airy beams appear simultaneously, and the quality of Airy beams needs to be improved. A suitably curved refractive element has been chosen to form the cubic phase [16], but it can only be applied in an optical system whose size is macroscale. Also, some groups have employed a combination of positive and negative cylindrical lenses of a specific curvature radius [17] or tilted cylindrical lenses system [18] for constituting the cubic phase. Nevertheless, the bulky cylindrical lenses increase the complexity of the Airy beam generating system.

Another simple means to generate Airy beams is modulating the Gaussian beam by cubic phase plates (CPPs). A CPP has been realized by using binary subwavelength microstructures [19], but the characteristic multilobed intensity pattern of the generated Airy beam is not evident, because the fabricated phase plate is not strictly cubic. Some researchers have fabricated continuous cubic phase plates in millimeter scale [20,21] using a laser direct writer (DWL66, Heidelberg Instruments). However, due to the low fabrication precision of the laser direct writer with a pixel of 30 μm, the generated Airy beam is defective, e.g., the main lobe and nearby side lobes are mixed together. In addition, limited by the size, these CPPs are not suitable for integrated optics, whose dimensions of components are usually in micrometer scale. Therefore, it is essential to fabricate CPPs with both micro size and continuous variation of phase.

The purpose of this Letter is to exquisitely design and fabricate a continuous cubic phase microplate (CCPP) for generating high-quality Airy beams. A square CCPP with an accurate length (60 μm) and height (1.1 μm) is fabricated via femtosecond laser direct writing (FsLDW), which has been widely used for fabricating arbitrary three-dimensional (3D) microdevices [22–25]. An Airy beam is experimentally realized via the precisely fabricated CCPP, and the properties of the generated Airy beam are investigated as well. The generated Airy beam exhibits an unprecedentedly strong deflection (the main lobe shifts about 4.2 μm within a 90 μm propagation distance), as well as being diffraction-free (the spot size of the main lobe remains almost unchanged during a 90 μm propagation).

It's known that the envelope of a finite Airy beam [1] is expressed as

$$\phi(\xi, s) = Ai[s - (\xi/2)^2 + ia\xi]\exp[as - (a\xi^2/2) - i(\xi^3/12) + i(a^2\xi/2) + i(s\xi/2)]. \quad (1)$$

Here $Ai[s - (\xi/2)^2 + ia\xi]$ represents the Airy function, a is a positive parameter for ensuring containment of the infinite Airy tail, $a \ll 1$, $s = x/x_0$ represents a dimensionless transverse coordinate, and x_0 is an arbitrary transverse scale. $\xi = z/kx_0$ is a normalized propagation distance, $k = 2\pi n/\lambda$ represents a wavenumber, n is the refractive index of the medium, and λ is the free space wavelength. For a two-dimensional (2D) case, the Fourier transform of the envelope is

$$\Phi_0(k_x, k_y) \propto \exp[-a(k_x^2 + k_y^2)]\exp[i(k_x^3 + k_y^3)/3, \quad (2)$$

where k_x and k_y are Fourier spectrum coordinates. As a result, an Airy beam can be generated from a Gaussian beam imposed by a cubic phase through a Fourier transformation. The cubic phase pattern, whose size is 600 pixels × 600 pixels, wrapped between 0 and 2π with the phase range varying from -16π to 16π according to $\varphi(x, y) = x^3 + y^3$ in the x–y plane, is shown in Fig. 1(a).

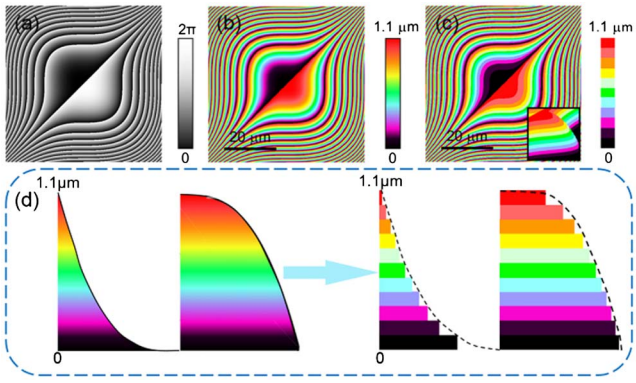

Fig. 1. Design of a CCPP. (a) Cubic phase pattern wrapped between 0 and 2π used to generate a 2D Airy beam. Size, 600 × 600 pixels; phase range, $-16\pi \sim 16\pi$. (b), (c) Images of designed CCPPs with continuous height and step-like height, respectively. Size, 60 μm × 60 μm × 1.1 μm. Inset in (c): Local 3D image. (d) Schematic of the discretization progress of a local structure of the CCPP with a layer separation of 100 nm; the dashed line represents the height profile after fabrication as a result of the self-smoothing effect of the photoresist.

Our design begins with converting the phase to the height using

$$h(x, y) = h_0\varphi(x, y)/2\pi, \qquad |x| \le L, |y| \le L, \quad (3)$$

where $L = 30$ μm is the half-length of a CCPP and $h_0 = \lambda_0/(n_0 - 1)$ is a constant once the wavelength of incident light λ_0 to generate the Airy beam and the refractive index of the material n_0 for fabrication are determined. A green light laser has $\lambda_0 = 532$ nm, while the photoresist [SZ-2080 (IESL-FORTH) mixed with 1 wt. % 4,4-Bis(diethylamino)benzophenone (BIS) with an absorption maximum at 368 nm (Sigma–Aldrich GmbH)], which is a good material for 3D micro/nanofabrication [26,27], has $n_0 = 1.5$, so $h_0 \approx 1.1$ μm, and each height in the x–y plane can be calculated using Eq. (3). The designed CCPP is shown in Fig. 1(b). Due to the precision of our FsLDW system [Fig. 2(a)], the height of the CCPP is segmented with a step of 100 nm. Our fabrication is carried out layer by layer, which causes the CCPP to be divided into 11 layers [Fig. 1(c)]. The height is discretized according to the following principle:

$$h = \begin{cases} 0, & 0 \le h < 50 \\ 100i \text{ nm}, & 50 + 100(i-1) \le h < 50 + 100i, \\ 1100 \text{ nm}, & 1050 \le h < 1100 \end{cases} \quad (4)$$

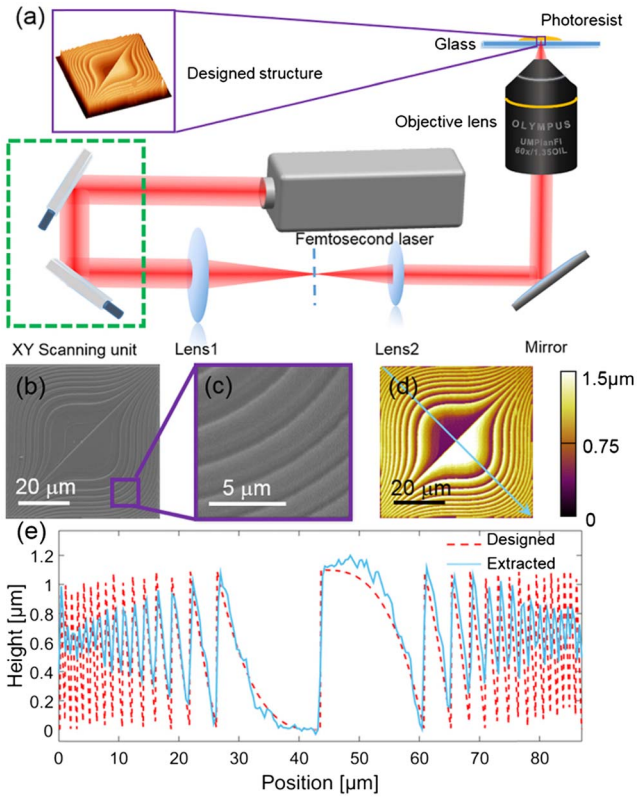

Fig. 2. Fabrication of the continuous cubic phase microplate (CCPP) by femtosecond laser direct writing (FsLDW). (a) Schematic of the experimental setup for the fabrication of the CCPP; (b) SEM micrograph of the fabricated CCPP; (c) locally magnified SEM micrograph of (b); (d) AFM image of the fabricated CCPP; (e) height profile with respect to the substrate (300 nm) along the diagonal line of the CCPP. The solid line represents the extracted profile marked in (d), while the dashed line represents the designed profile.

where $i = 1, 2, \ldots, 10$ denotes the number of the layer, and the discretization progress of local structure is illustrated in Fig. 1(d).

The CCPP was fabricated by focusing the femtosecond laser beam (Coherent Chameleon Vision-S, 80 MHz repetition rate, 800 nm center wavelength, and 75 fs pulse width) into the photoresist using a 60 × oil immersion objective lens with a numerical aperture (NA) of 1.35 [Fig. 2(a)], and the exposing power was set to 8 mW. The fabrication process in each layer was controlled by a pair of scanning galvo mirrors, while the step between two layers was realized by a nano-positioning stage. Thanks to the self-smoothing effect of the photoresist [28], the structure tends to be continuous and smooth after fabrication in the course of unpolymerized resin rinsing [dashed line in Fig. 1(d)], so there is no need to worry about the step-like fabrication. Scanning electron microscopy (SEM; FEI Sirion200) micrographs shown in Figs. 2(b) and 2(c) illustrate our precise fabrication of the CCPP.

In order to investigate the topography of our structure, the CCPP was characterized by an atomic force microscope (AFM; MFP3D-origin OXFORD, Cantilever: Tap300Al-G, tapping mode), as shown in Fig. 2(d). The CCPP was fabricated on a substrate with height of 300 nm to ensure the integrity of the cubic phase. The surface morphology of the CCPP is considered a significant factor in our fabrication; therefore, we extracted the height profile of the CCPP relative to the substrate along the diagonal marked in Fig. 2(d). The extracted height matches well with the designed height, as shown in Fig. 2(e), and the small difference between the designed and the measured height profile may be caused by fabrication or measurement errors. Some small waves, especially in the center of the CCPP, are caused by the distortion of the photoresist during fabrication and development, which is unavoidable in the micro/nano scale. It is also necessary to explain that some spacing between adjacent crescent-shaped structures is so tiny that the AFM probe can't dip to the bottom, which causes mismatching between the extracted height and the designed one far away from the center of the CCPP. The farther the crescent-shaped structure is from the center, the smaller the gaps become, and the less accurate the result of the AFM is. So the mismatching is unavoidable due to the high aspect ratio of local areas.

To characterize the performance of the CCPP, a series of tests have been carried out. A 2D Airy beam was experimentally generated via the CCPP from a Gaussian beam through Fourier transformation by a 40 × objective lens (NA = 0.6) with a focal length of 180 μm and was recorded by a charge-coupled device (CCD) camera at different propagation planes. The cw laser beam (532 nm, 1 mW) was truncated through an aperture to ensure a small beam width (~100 μm), since the length of the CCPP is 60 μm. Figure 3(a) depicts the 2D Airy beam observed at the Fourier plane generated via our fabricated CCPP. The characteristic multilobed intensity pattern of the Airy beam is distinct in the image, while the full width at half-maximum (FWHM) of the main lobe is about 2.7 μm, which is coincident with the simulated result [Fig. 3(a) inset]. Compared to Airy beams generated through other fabricated CPPs whose phase profiles are not strictly cubic, the Airy beam generated through the CCPP exhibits relatively high quality. To clearly characterize the intensity distribution of the generated 2D Airy beam, a 3D view of the optical distribution is

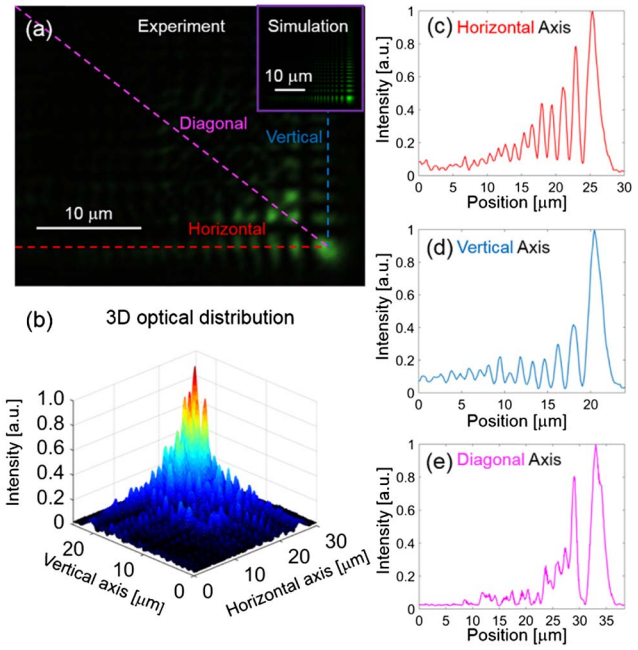

Fig. 3. Observation of the Airy beam generated via the CCPP. (a) Experimental micrograph of the 2D Airy beam with the 2.7 μm FWHM of the main lobe, which is in good agreement with the simulated one (inset); (b) 3D optical distribution of (a); (c)–(e) normalized intensity along the horizontal, vertical, and diagonal axes, respectively, marked with dashed lines in (a).

presented in Fig. 3(b). Figures 3(c)–3(e) depict the corresponding intensity profiles along the horizontal, vertical, and diagonal axes, respectively, marked with dashed lines in homologous colors. As expected, the main lobe has the highest intensity, while the intensity of other lobes drops rapidly.

Optical efficiency of the CCPP was detected as well, and it is defined as the rate of laser power measured behind the CCPP on a glass substrate, divided by the laser power coming from the laser source. Figure 4(a) illustrates the relationship between optical efficiency and laser power. We can see that the efficiency, with a mean of 79%, is fairly stable and just fluctuates slightly from 77% to 81%, with the laser power varying from 1 mW to 7 mW. Due to the possible unstable factors during the fabrication and development process, the final morphology of the CCPP is not perfectly as-designed, which makes the efficiency a little lower. The CCPP is fabricated on a glass substrate, and as a result, there is inevitably a partial transmission loss from the glass, around 12%.

As reported in Ref. [6], the transverse deflection can be approximately expressed using a quadratic function:

$$D(z) = 3.7 \times 10^{-2}(\lambda_0^2/W_A^3) \times z^2, \tag{5}$$

where λ_0 is the wavelength of the incident light to generate the Airy beam, W_A is the FWHM of the main lobe at the Fourier plane, and z is the propagation distance after the Fourier plane. In Eq. (5), the deflection $D(z)$ is mainly affected by the FWHM W_A, which can be controlled by the focal length of the lens. With objective lens focusing, we obtain a micro-size Airy beam with a 2.7 μm FWHM of the main lobe

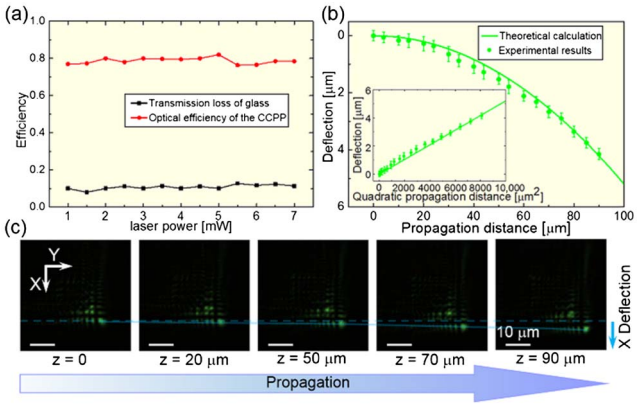

Fig. 4. Characterization of the Airy beam. (a) Relationship between optical efficiency of the CCPP and laser power, (b) transverse acceleration of the Airy beam as a function of beam propagation distance. Inset: Linearization of the transverse acceleration of the Airy beam via squaring the propagation distance. (c) Images of the generated Airy beam observed at various propagation planes. The blue solid line represents the deflection in the x direction.

[Fig. 3(a)] and a strong deflection. The transverse shift of the generated Airy beam can be calculated from the images taken by a CCD camera at various propagation distances. Figure 4(b) depicts the transverse acceleration of the Airy beam as a function of beam propagation distance. Our results show an unprecedentedly strong deflection with a transverse shift of 4.2 μm after a 90 μm propagation. This value is larger than any other reported results that we know of because of the smaller focal length of the Fourier transform utilized in our experiment. In addition, our experimental results [green points in Fig. 4(b)] show good agreement with the theoretical calculation [green line in Fig. 4(b)]. As predicted, after the propagation distance is squared, the linear behavior clearly emerges, as shown in the inset of Fig. 4(b).

The nondiffraction properties of the generated Airy beam were verified as well. Figure 4(c) shows some images of the generated Airy beam taken at different propagation planes, and the acceleration trajectory in the x direction, which is same as the one in the y direction, is marked with a blue solid line. As we can see, the spot size of main lobe remains almost unchanged during a 90 μm curved propagation. Therefore, the CCPP can be utilized to generate a high-quality Airy beam in micrometer scale, similar to a macro-size CPP.

In conclusion, we have elaborately designed and fabricated a CCPP by FsLDW with precise size (60 μm × 60 μm × 1.1 μm). This miniature phase component is the critical factor in generating high-quality Airy beams, showing an optical efficiency up to 79% (much higher than SLMs), which can be helpful in integrated micro-optics. An Airy beam generated via the CCPP under a wavelength of 532 nm has been observed, which coincides well with the theoretical simulation. Typical properties such as nondiffraction and transverse acceleration characteristics have been experimentally verified as well. The generated Airy beam shows an extremely strong transverse shift (~4.2 μm within a 90 μm propagation distance). This work can provide a universal approach to designing and fabricating complex elements for beam shaping, microscopy, and high-performance optical manipulation on a micrometer scale.

Funding. National Natural Science Foundation of China (NSFC) (51405464, 51605463, 51675503, 61475149, 61675190); Fundamental Research Funds for the Central Universities (WK2480000002); China Postdoctoral Science Foundation (2016M590578, 2016M602027); Chinese Academy of Sciences (CAS) Instrument Project (YZ201566); Chinese Thousand Young Talents Program.

REFERENCES

1. G. A. Siviloglou, J. Broky, A. Dogariu, and D. N. Christodoulides, Phys. Rev. Lett. **99**, 213901 (2007).
2. G. A. Siviloglou and D. N. Christodoulides, Opt. Lett. **32**, 979 (2007).
3. J. Baumgartl, M. Mazilu, and K. Dholakia, Nat. Photonics **2**, 675 (2008).
4. P. Zhang, J. Prakash, Z. Zhang, M. S. Mills, N. K. Efremidis, D. N. Christodoulides, and Z. G. Chen, Opt. Lett. **36**, 2883 (2011).
5. D. Abdollahpour, S. Suntsov, D. G. Papazoglou, and S. Tzortzakis, Phys. Rev. Lett. **105**, 253901 (2010).
6. P. Polynkin, M. Kolesik, J. V. Moloney, G. A. Siviloglou, and D. N. Christodoulides, Science **324**, 229 (2009).
7. A. Salandrino and D. N. Christodoulides, Opt. Lett. **35**, 2082 (2010).
8. A. Minovich, A. E. Klein, N. Janunts, T. Pertsch, D. N. Neshev, and Y. S. Kivshar, Phys. Rev. Lett. **107**, 116802 (2011).
9. A. Mathis, F. Courvoisier, L. Froehly, L. Furfaro, M. Jacquot, P. A. Lacourt, and J. M. Dudley, Appl. Phys. Lett. **101**, 071110 (2012).
10. N. Voloch-Bloch, Y. Lereah, Y. Lilach, A. Gover, and A. Arie, Nature **494**, 331 (2013).
11. S. Jia, J. C. Vaughan, and X. Zhuang, Nat. Photonics **8**, 302 (2014).
12. T. Vettenburg, H. I. C. Dalgarno, J. Nylk, C. Coll-Llado, D. E. K. Ferrier, T. Cizmar, F. J. Gunn-Moore, and K. Dholakia, Nat. Methods **11**, 541 (2014).
13. Z. Zhang, Z. You, and D. Chu, Light Sci. Appl. **3**, e213 (2014).
14. H. T. Dai, X. W. Sun, D. Luo, and Y. J. Liu, Opt. Express **17**, 19365 (2009).
15. D. Luo, H. T. Dai, and X. W. Sun, Opt. Express **21**, 31318 (2013).
16. A. Valdmann, P. Piksarv, H. Valtna-Lukner, and P. Saari, Opt. Lett. **39**, 1877 (2014).
17. B. Yalizay, B. Soylu, and S. Akturk, J. Opt. Soc. Am. A **27**, 2344 (2010).
18. D. G. Papazoglou, S. Suntsov, D. Abdollahpour, and S. Tzortzakis, Phys. Rev. A **81**, 061807 (2010).
19. M. S. Mirotznik, J. van der Gracht, D. Pustai, and S. Mathews, Opt. Express **16**, 1250 (2008).
20. R. Cao, Y. Yang, J. Wang, J. Bu, M. Wang, and X. C. Yuan, Appl. Phys. Lett. **99**, 261106 (2011).
21. J. G. Wang, J. Bu, M. W. Wang, Y. Yang, and X. C. Yuan, Appl. Opt. **50**, 6627 (2011).
22. H. Xia, J. Wang, Y. Tian, Q. D. Chen, X. B. Du, Y. L. Zhang, Y. He, and H. B. Sun, Adv. Mater. **22**, 3204 (2010).
23. L. Jiang, W. Xiong, Y. Zhou, Y. Liu, X. Huang, D. Li, T. Baldacchini, L. Jiang, and Y. Lu, Opt. Express **24**, 13687 (2016).
24. M. Malinauskas, A. Žukauskas, S. Hasegawa, Y. Hayasaki, V. Mizeikis, R. Buividas, and S. Juodkazis, Light Sci. Appl. **5**, e16133 (2016).
25. T. Gissibl, S. Thiele, A. Herkommer, and H. Giessen, Nat. Photonics **10**, 554 (2016).
26. M. Malinauskas, P. Danilevicius, and S. Juodkazis, Opt. Express **19**, 5602 (2011).
27. L. Jonušauskas, D. Gailevičius, L. Mikoliūnaitė, D. Sakalauskas, S. Šakirzanovas, S. Juodkazis, and M. Malinauskas, Materials **10**, 12 (2017).
28. K. Takada, H.-B. Sun, and S. Kawata, Appl. Phys. Lett. **86**, 071122 (2005).